Computational Materials Science 163 (2019) 100–107

Contents lists available at ScienceDirect

Computational Materials Science

journal homepage: www.elsevier.com/locate/commatsci

Influence of bulk free energy density on single void evolution based on the phase-field method

Yang Li[a,b], Decai Ma[a,*], Biao Wang[a,c,d,*]

[a] Sino-French Institute of Nuclear Engineering and Technology, Sun Yat-sen University, Zhuhai 519082, China
[b] DEN-Service de Recherches Métallurgiques Appliquées, CEA, Université Paris-Saclay, Gif-sur-Yvette 91191, France
[c] State Key Laboratory of Optoelectronic Materials and Technologies, Sun Yat-sen University, Guangzhou 510275, China
[d] School of Physics, Sun Yat-sen University, Guangzhou 510275, China

ARTICLE INFO

Keywords:
Phase-field method
Void growth rate
Interface width

ABSTRACT

Phase-field models are widely adopted to study the void evolution problem, overcoming difficulties and drawbacks of the sharp boundary approach and rate theory. This paper focuses on improving the performance of the phase-field model of which the vacancy concentration is used as the single conserved order parameter. Following recent developments in these phase-field models, the void dynamic, or more precisely the void growth rate which plays a vital role in characterizing the microstructural evolution of irradiated materials, cannot be accurately reproduced. Moreover, the interfacial energy or the void-matrix interface modeled by the Ginzburg-type gradient energy term is usually characterized by an empirical coefficient that is quite difficult to determine. For these reasons, a general relation of the bulk free energy density, the coefficient of the gradient energy term and the interface width is analytically derived from the planar interface case, and then validated by the numerical simulation example of a single void evolution in molybdenum (Mo). The obtained void growth rate agrees well with the prediction of rate theory while the interface width is smaller than a critical value in the considered cases regardless of the shape of the free energy density. This study will not only help to construct the appropriate formulation of the bulk free energy density, but will also provide an easy method of calculating the corresponding gradient energy coefficient and selecting the grid size according to the pre-estimated interface width.

1. Introduction

Under long-time exposure of energetic particle radiation, numerous Frenkel pairs, i.e. vacancies and self-interstitials, are generated in irradiated materials. Regardless of the recombination, due to the fast diffusion, the interstitials are much easily trapped by the sinks such as dislocations and grain-boundaries, which results in more surviving vacancies. This process is known as production bias [1–4]. These supersaturated vacancies can freely migrate inside a crystalline solid, and then either be trapped by the sinks or cluster together to form the nucleus of the void. A nucleus with a small radius containing just a few vacancies is generally not stable and dissolves immediately. However, because of the continuous generation of additional vacancies and their diffusion, a void with a sufficiently large radius occasionally forms and grows by absorbing more vacancies. This long-term evolution is known as void nucleation and growth [5–7].

The aforementioned process can cause volumetric swelling (a decrease in the density), a reduction of the Young's modulus, a decrease in plasticity and a change in the yield stress of the structural materials in nuclear reactor [8–11], which may significantly affect the mechanical properties and the life-times of these components. In this context, the void growth rate, generally used to quantify the void evolution behavior, therefore plays a vital role in characterizing the microstructural evolution of irradiated materials. The mechanical understanding of these material degradations can help to design high irradiation-resistant materials for nuclear reactor components [12,13].

The void growth can be simply described using the following chemical-reaction-like process:

$$n\mathrm{V} + \mathrm{Void}_m \rightleftharpoons \mathrm{Void}_{m+n}.$$

where V denotes the vacancy. Physically, the bulk containing vacancies with supersaturated concentration is thermally unstable. Therefore, as shown in Fig. 1, the existing void with a radius R that is a physical vacuum space with zero vacancy concentration, acts as a sink for absorbing the supersaturated vacancies. Neglecting the mechanical drift

---

[*] Corresponding authors at: Sino-French Institute of Nuclear Engineering and Technology, Sun Yat-sen University, Zhuhai 519082, China (D. Ma and B. Wang).
E-mail addresses: madecai@mail.sysu.edu.cn (D. Ma), wangbiao@mail.sysu.edu.cn (B. Wang).

https://doi.org/10.1016/j.commatsci.2019.03.014
Received 17 December 2018; Received in revised form 7 March 2019; Accepted 8 March 2019

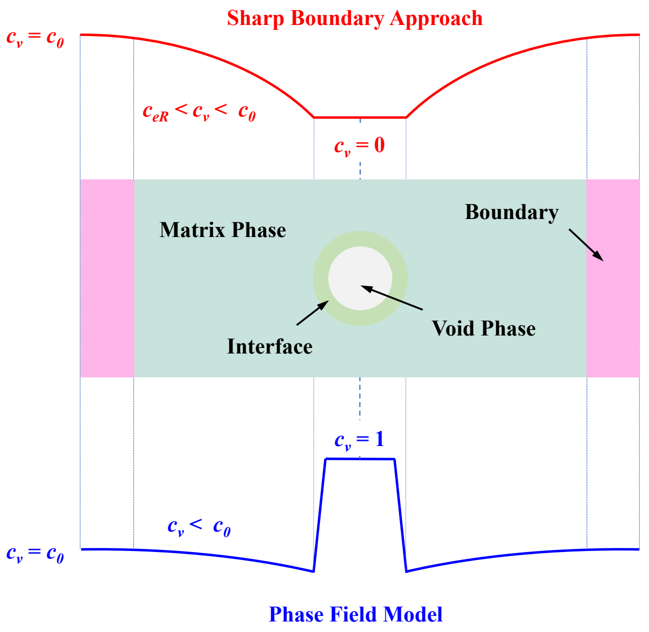

Fig. 1. Physical model of void growth (center), with illustrations of the vacancy concentration profile in the sharp boundary approach (top) and the phase-field model (bottom).

of the void strain field to the vacancies, the point defect concentration gradient is the only driving force governing such process. Because of the sharp interface between the bulk and the void, the corresponding interfacial tension, acting as the drag force, effectively reduces the flux of vacancies towards the void. This is a typical unbiased diffusion-controlled reaction process.

For an isotropic crystal, it can be simplified as a spherical system with a single void located at the center that is surrounded by bulk crystal with initial (and boundary) vacancies concentration c_0. Following the reaction rate theory (RT) which is based on mean-field approximation, the void growth rate can be calculated by the increasing rate of the void radius $R = R(t)$ as [12,14,15]

$$\frac{\mathrm{d}R}{\mathrm{d}t} = D[c_0 - c_{eR}]\frac{L}{(L-R)R} \tag{1}$$

where D is the vacancy diffusion coefficient and $D = D_0\exp(-E^m/k_\mathrm{B}T)$, where D_0 is the vacancy diffusivity pre-exponential, E^m is the vacancy migration energy, k_B is Boltzmann's constant, and T is the absolute temperature. L is the dimension of the spherical domain containing supersaturated vacancies and c_{eR} is the thermal equilibrium concentration of the vacancy solution in presence of the void with radius R, which is expressed as

$$c_{eR} = \exp[-(E^f - E(R))/k_\mathrm{B}T] = c_e b(R) \tag{2}$$

where $c_e = \exp(-E^f/k_\mathrm{B}T)$ is the vacancy equilibrium concentration (without the presence of the void). E^f is the formation energy and $b(R) = \exp(E(R)/k_\mathrm{B}T)$ characterizes the resistant effect due to the interfacial tension, determined by $E(R) = 2\gamma_s\Omega/R$, where γ_s is the surface tension and Ω is the atomic volume of the metal. Eq. (1) under the mean-field approximation could provide only average spatial information on the void growth. Originally proposed by Gibbs [16] to emulate the phase transition and micro-structural evolution in crystalline solids, the sharp interface approach (SBA) was developed to achieve the spatial resolution, wherein a set of differential equations are used to describe the void nucleation and growth with a zero-thickness interface between the void and matrix phases, i.e. the sharp boundary [17,18]. However, the requirement for tracking the instantaneous position of the moving interface has some numerical difficulties, especially in case with complicated phase morphology. In this regard, the phase-field model (PFM) with a diffusive boundary was widely adopted to overcome the drawbacks of the sharp boundary approach for modelling the phase separation, of which the temporal evolution of a spatial-related order parameter c is solved from the time-dependent Ginzburg-Landau equation [19–25]. The description of the diffuse interface results in a continuous distribution of such order parameter, and therefore no need for the specific treatment on the interface position.

The PFM has been beneficial for studying the phase separation of binary alloy systems, where the spatial-related order parameter has been chosen as the concentration of the involved element. In 1978, Imada [26] promoted the PFM for void evolution by choosing the spatial-dependent vacancy concentration $c(x, t)$ as the order parameter, and setting $c = 1$ and $c \approx 0$, respectively, to denote the void phase and the bulk phase with no interstitial involvement. While in recent years, other phase-field models with different sets of order parameters have been developed which also provide excellent performances in modelling void nucleation and growth [27–29], the former model has pronounced advantages. For instance, only one differential control equation, namely the Cahn-Hilliard equation, is required to be solved. It is simple to implement and exhibits efficiency in numerical calculations of much more complex systems such as evolutions of void ensembles (for more details, see [22,30]). Therefore, this paper focuses on studying the phase-field model where the vacancy concentration is the single order parameter.

However, these benefits come at the cost of having to deal with a number of difficulties. For example, the definition of the vacancy concentration inside the void, $c = 1$, conflicts with physical reality. Also, to emulate the void evolution, the initial supersaturated vacancy concentration in the matrix is usually set several orders of magnitude above the corresponding thermal equilibrium value, e.g. $c \sim 10^{-3}$ (atomic fraction) or even higher [22,31,23], which is thus far beyond the limit of the dilute and ideal solution. In addition, applying the spinodal decomposition of the phase separation to describe the void nucleation process is another problem. Some mathematical modifications are thus necessary to guarantee that the quantitative results are consistent with the experimental observations and the predictions of other well-established models. As such, Semenov et al. [30,32,33] recently proposed an improved PFM by deriving the free energy from the limit of the dilute solution condition based on the classical nucleation theory, of which the static solution agrees with experimental observations. Following this PFM, Xiao et al. [15] performed a dynamic simulation of a single void evolution with the same dilute vacancy concentration. However, their average void growth rate, which is an essential parameter used to characterize the void evolution kinetic, had a large relative error above 30% (several cases achieved 100%) compared to the referent prediction of rate theory. A 30% relative error may cause a 30% overestimation of the swelling rate, which in turn results in a significant overestimation of the decrease in plasticity of irradiated materials (for instance, more than two times for highly irradiated austenitic steels [9,10]). This kind of numerical error can usually be reduced by tuning the surface tension. Unfortunately, this does not always work, particularly at relatively low temperatures where the void evolution is only slightly affected by the vacancy emission. In this circumstance, in order to correctly and accurately reproduce the void dynamic without tuning any material parameters, gaining a more general understanding of the difference between the PFM and rate theory is desired. Additionally, in the phase-field framework, the interfacial energy associated with the void-matrix interface is modeled by a Ginzburg-type gradient energy term. This term is usually characterized by a coefficient using the empirical value or derived from other assumptions. However, much uncertainty still exists about the relation between this gradient energy coefficient and the physics of the interface. Hence, identifying its role and deducing a simple formula for this quantity are further purposes of this work.

In this paper, we will first analyze the relation of the free energy density, the coefficient of the gradient energy term and the interface width of the former phase-field model, and then assess the factors resulting in the gap of the void growth rate obtained from the PFM and RT. The paper is organized as follows: the theoretical analysis is presented in Section 2; the numerical simulation example of BCC Mo for a single void system is performed in Section 3 to check our conjectures; and the conclusion is presented in Section 4.

2. Dilute phase-field model for void growth

2.1. General framework of the phase-field model

As shown in Fig. 1, the void growth in the PFM is in analogy to the phase separation of a binary alloy where the vacancy concentration c is regarded as a single conserved variable, solved from the Cahn-Hilliard equation [34–36], i.e.

$$\frac{\partial c(\boldsymbol{r},t)}{\partial t}=\Omega\nabla\left\{M\nabla\frac{\delta F[c(\boldsymbol{r},t)]}{\delta c(\boldsymbol{r},t)}\right\}\equiv\nabla[M\nabla\mu(\boldsymbol{r},t)] \tag{3}$$

where $F[c]$ is the free energy of the vacancy concentration and M is the vacancy mobility, usually defined as [33]

$$M=\frac{D}{k_{\mathrm{B}}T}c(1-c) \tag{4}$$

where D is the diffusivity of vacancy holding the same temperature-dependent expression as in Eq. (1) and μ is the chemical potential,

$$\mu(\boldsymbol{r},t)=\Omega\frac{\delta F[c(\boldsymbol{r},t)]}{\delta c(\boldsymbol{r},t)} \tag{5}$$

To obtain the phase-separation in the PFM, the free energy is usually written as

$$F[c]=\frac{k_{\mathrm{B}}T}{\Omega}\int_V[f[c(\boldsymbol{r})]+\varkappa^2(\nabla c)^2]\mathrm{d}\boldsymbol{r} \tag{6}$$

where $f[c(\boldsymbol{r})]$ is defined as a dimensionless reduced bulk free energy density, and $\varkappa^2(\nabla c)^2$ is the Ginzburg-type gradient energy term, arising from the inhomogeneous nature of the concentration distribution, resulting in the so-called diffusive interface boundary between the void and matrix phases. Substituting Eq. (6) into Eq. (3), the evolution of the order parameter is given by

$$\frac{\partial c(\boldsymbol{r},t)}{\partial t}=\nabla\left[k_BTM\nabla\left(\frac{\mathrm{d}f}{\mathrm{d}c}-2\varkappa^2\Delta c\right)\right] \tag{7}$$

From Eq. (7), it is easy to see that the evolution of the order parameter is mainly determined by the functional form of the bulk free energy density $f[c(\boldsymbol{r})]$ and the gradient energy coefficient $\varkappa$. In this regard, the void growth could be characterized by the increase in the void radius associated with the vacancy-flux towards the void [15,30]

$$R(t)=\left[3\int_0^{r_{min}}r^2c(\boldsymbol{r},t)\mathrm{d}r\right]^{\frac{1}{3}} \tag{8}$$

where r_{min} is the spatial position of the local minimum of the vacancy concentration. Therefore, the void growth rate $\Gamma(t)$ is estimated by $\Gamma(t)=\dot{R}(t)$. Since outside of the void, the concentration is very small, possible alternative definitions will have little influence on such void radius, which has been examined in Ref. [15].

2.2. Dilute formulation of the bulk free energy density

In Eq. (7), the bulk free energy density f provides the local driving force in terms of a gradient against the order parameter in phase-space. The functional formulation of the free energy density was not unique in the literature, as long as some conditions were satisfied: the free energy density profile should be a double-well potential, with two local minima corresponding to the stable phases and one local maximum. In the void growth problem, for example,

$$\begin{cases}\frac{\partial f}{\partial c}=0\quad\text{and}\quad\frac{\partial^2 f}{\partial c^2}>0, & \text{when}\quad c=c_e\\ \frac{\partial f}{\partial c}=0\quad\text{and}\quad\frac{\partial^2 f}{\partial c^2}<0, & \text{when}\quad c=c_m\in[c_e,1]\\ \frac{\partial f}{\partial c}=0\quad\text{and}\quad\frac{\partial^2 f}{\partial c^2}>0, & \text{when}\quad c=1\end{cases} \tag{9}$$

where $c=c_e$ corresponds to the bulk crystal phase, with c_e representing the temperature-dependent equilibrium vacancy concentration in matrix and $c=1$ for the void phase, where the vacancy concentration approaches unity. $f[c_m]$ is a local maximum, indicating a potential barrier for the phase separation, and c_m is the location of the potential maximum. The formulation of $f=f[c]$ is generally set to obey the conditions in Eq. (9), but its relationship with the classical nucleation theory is not well considered, resulting in the so-called spinodal decomposition and the requirement of a very high initial vacancy concentration in the matrix solution, as mentioned in Section 1. To solve this problem, Semenov et al. [30,32] proposed the formulation of $f=f[c]$ based on the ideal dilute solution

$$f[c]=c\left[\ln\left(\frac{c}{c_e}\right)-1\right]-\varphi_n[c] \tag{10}$$

Here, the first term in *rhs* of Eq. (10) corresponds to the free energy density in the dilute limit, and $\varphi_n(c)$ is the correction of f deviated from the dilute solution limit at $c\gg c_e$, written as

$$\begin{aligned}\varphi_n[c]=&-[n\ln c_e+(n+1)(1-c_0)]c^n\\&+[(n-1)\ln c_e+n(1-c_0)]c^{n+1}\quad(n\geqslant 2)\end{aligned} \tag{11}$$

The presence of the correction term $\varphi_n[c]$ provides a channel to adjust the magnitude of the local maximum, as shown in Fig. 2(a) with $n=2.0$, 2.5, 3.0, 4.0 and 5.0 plotted. As aforementioned, the functional formulation of $f=f[c]$ is not unique. For instance, Xiao et al. [15] proposed another formulation as

$$f[c]=c\ln c+(1-c)\ln(1-c)+\frac{E^f}{k_BT}c(1-c) \tag{12}$$

which also meets the dilute and ideal solution requirement and the conditions in Eq. (9). Therefore, a large number of free energy density forms can be chosen, which results in different void dynamics.

2.3. Gradient term and diffusive interface width

The gradient term in Eq. (6) describes the action of non-uniform vacancy concentration in the phase-field model, with the coefficient $\varkappa$ characterizing the formation of the diffusive field. In general, $\varkappa$ depends on the void size, the metallic surface tension γ_s, and the bulk free energy density. However according to Ref. [30], $\varkappa$ is almost independent of the void size, so that it could be directly expressed as

$$\varkappa=\frac{\Omega\gamma_s}{2k_BT}\left[\int_{c_e}^1\sqrt{f[c]+c_e}\,\mathrm{d}c\right]^{-1}=\frac{\Omega\gamma_s^*}{2k_BT} \tag{13}$$

where γ_s^* is the effective surface tension with respect to the free energy profile $f[c]$, as

$$\gamma_s^*=\gamma_s/I(c_e) \tag{14}$$

and

$$I(c_e)=\int_{c_e}^1\sqrt{f[c]+c_e}\,\mathrm{d}c \tag{15}$$

In fact, the above expression is derived based on the classical nucleation theory by equaling the variation of the free energy in terms of the void nucleation to the interfacial energy. Therefore, $\varkappa$ is coupled with the adopted free energy density in this model. However in previous studies, the coefficient $\varkappa$ is selected as an empirical constant or obtained from Eq. (13) by assuming $I=1$. This implementation may lead to a deviation in the nucleation process from the classical nucleation theory and therefore is not robust for numerical modeling. This expression thus needs to be discussed in detail. It is worth to note that if the functional form of $f[c]$ satisfies the former conditions expressed in Section 2.2, e.g. Eq. (10) or (12), the term in the integral I will always possess two roots at $c \approx c_e$ and $c \approx 1$, owing to the ideal dilute limit where $f[c_e] = -c_e$, and a local maximum $\sqrt{f_{max} + c_e}$ around $c \sim 0.5$ (see also Fig. 2(a)), where $f_{max} \equiv f[c_m]$. Since c_e is quite small, solving the former integration could be approximately regarded as calculating the integral of a second order polynomial,

$$\begin{aligned} I &= \int_{c_e}^{1} \sqrt{f[c] + c_e}\ \mathrm{d}c \\ &\approx \int_{c_e}^{1} -4\sqrt{f_{max}}\ (c - c_e)(c - 1)\mathrm{d}c \\ &= \tfrac{2}{3}\sqrt{f_{max}} \end{aligned} \tag{16}$$

Substituting Eq. (16) into Eq. (13), it gives

$$\varkappa = \frac{\Omega\gamma_s^*}{2k_{\mathrm{B}}T} = \frac{\Omega\gamma_s}{2k_{\mathrm{B}}T}\left[\frac{2}{3}\sqrt{f_{max}}\right]^{-1} \tag{17}$$

Eq. (17) is a main result of this paper, predicting that the gradient energy coefficient $\varkappa$ is inversely proportional to the square root of the local maximum, independent of the free energy density's shape. Indeed, rather than depending on γ_s, the $f[c]$ weighted γ_s^* is one key term to characterize the vacancy emission ability of void across the void-matrix phase boundary and thus the void growth rate. As previously discussed, another validation of this expression is in the aspect of the void nucleation characterized by the critical size of the void R_{cr}, which determines the shrinkage or the growth of the void and corresponds to the maximal change in the free energy during the void nucleation process. Higher f_{max} induces smaller γ_s^* and then results in less requirement of the free energy variation thus smaller R_{cr}, which is consistent with the classical nucleation theory. On the other hand, for the sake of clearly identifying its effect on the void growth process, the interface width Δl, which plays a vital role in evaluating the interface diffusivity, will be analyzed as follows.

Considering a single void system with an infinite large dimension, the evolution equation, i.e. Eq. (7) at the steady-state with $\partial c/\partial t = 0$ could be simplified as

$$\frac{\mathrm{d}f}{\mathrm{d}c} - 2\varkappa^2\Delta c = \ln\left(\frac{c_0}{c_e}\right) \tag{18}$$

where c_0 is the supersaturated vacancy concentration at $r \to \infty$. Multiplying the above equation by $\mathrm{d}c$ at each side then integrating from infinity yields

$$f[c] - f[c_0] - \varkappa^2(\nabla c)^2 = (c - c_0)\ln\left(\frac{c_0}{c_e}\right) \tag{19}$$

As it has already been proved that $\varkappa$ and the interface width are weakly dependent on the void radius, the planar interface case is assumed for simplicity. Taking $c_0 = c_e$, it gives

$$\varkappa^2(\nabla c)^2 = f[c] + c_e \tag{20}$$

where $f[c_0] = f[c_e] = -c_e$ according to the dilute solution condition. The readers should note that the vacancy concentration varies significantly within the interface, which separates the matrix phase and the void phase. The interface width Δl thus can be derived from the above equation by integrating it across the diffusive field, which gives

$$\Delta l = \int \mathrm{d}r = \int_{c_e}^{1} \frac{\varkappa}{\sqrt{f[c] + c_e}}\ \mathrm{d}c \tag{21}$$

Since $\varkappa$ is independent of the vacancy concentration, we expand Eq. (21) in Taylor series around the site $c = c_m$ where $f[c]$ reaches the maximal f_{max} and assuming $f_{max} > 1$, so that

$$\begin{aligned} \Delta l &= \varkappa \int_{c_e}^{1}\left[\frac{1}{[f_{max} + c_e]^{1/2}} - \frac{1}{2}\frac{1}{[f_{max} + c_e]^{3/2}} + \cdots\right]\mathrm{d}c \\ &= \varkappa\left[\frac{c - c_m}{[f_{max} + c_e]^{1/2}} - \frac{1}{4}\frac{(c - c_m)^2}{[f_{max} + c_e]^{3/2}} + \cdots\right]_{c_e}^{1} \\ &= \varkappa\left[\frac{1}{\sqrt{f_{max}}} + O\left(\frac{c_m}{f_{max}}\right)\right] \\ &\approx \frac{\Omega\gamma_s}{2k_{\mathrm{B}}T}\left[\frac{2}{3}f_{max}\right]^{-1} \end{aligned} \tag{22}$$

Based on the above equation, the interface width can be calculated using only the material parameters and the potential height, regardless of the vacancy concentration profiles. In addition, from Eq. (17) and Eq. (22), increasing the potential height first results in a smaller coefficient of the gradient energy term, and then they both contribute to reducing the interface width. Consequently, the evolution of the order parameter $c(\boldsymbol{r}, t)$ and thus the void growth rate are determined by the detailed information of the free energy density profile $f[c]$, or more explicitly its maximum value, i.e. $f_{max} = f[c_m]$.

To summarize, the validity of phase-field model implemented in the void evolution problem requires to construct the appropriate functional form of the free energy, expressed in terms of the bulk free energy density and the gradient energy term, which should satisfy the following conditions: the dilute solution condition, the correct nucleation process and the proper width of the diffusive interface to ensure the accurate void dynamic. Here, the two former conditions are solved by Semenov and the model is consistent with the classical nucleation theory. The latter could be solved by adjusting the barrier value f_{max} of the bulk free energy density. Moreover, the above expressions provide solutions to another problem mentioned in Section 1: (1) instead of using the empirical value or any other complicated expressions, the gradient energy coefficient $\varkappa$ can be easily calculated from Eq. (17); (2) the pre-estimated interface width from Eq. (22) helps to design the numerical code and to select the optimal grid size.

In the following, a numerical simulation example is performed by considering the single void growth in BCC Mo to further validate the aforementioned approach.

3. Numerical simulation: void growth in BCC Mo

In this section, for the sake of gaining a direct comparison with the results from Ref. [15], the identical simulation cell, i.e. a spherical domain with radius of $L = 11.8\,\mathrm{nm}$ is adopted and the coordinate system origin lies at the center of the cell. A single spherical void with the initial radius R_{init} is then placed at the position of $r = 0$, which corresponds to the typical void number density ($\sim 10^{23}\,\mathrm{m}^{-3}$) for molybdenum [37,38]. As such, modelling the void evolution reduces to one-dimensional problem along the radial direction of the simulation cell.

To emulate the real experimental condition, the homogeneous supersaturated vacancy concentration in the Mo matrix is initially set at c_0 ($10^{-8} \sim 10^{-7}$), and the initial conditions are written as

$$c(r, t = 0)|_{r \leqslant R_{init}} = 1, \quad c(r, t = 0)|_{R_{init} < r \leqslant L} = c_0 \tag{23}$$

Eq. (7) is fourth order in the spatial coordinates, and therefore four boundary conditions are taken as

$$\begin{aligned} &\nabla c(r, t)|_{r=0} = 0, \quad c(r, t)|_{r=L} = c_0 \\ &\Delta c(r, t)|_{r=L} = 0, \quad \nabla[\Delta c(r, t)]|_{r=L} = 0 \end{aligned} \tag{24}$$

Please note that the vacancy concentration at the volume boundary is assumed to be fixed and the last two conditions in Eq. (24) mean that far away from the void, both the chemical potential of the vacancies and their flux are independent of the void-matrix interface characteristics. Therefore, by introducing the diffusive interface in PFM, the void and the matrix can be uniformly treated through the continuous distribution of the vacancy concentration.

The temperature T is set around 1100 K to ensure that the void

Table 1
Simulation and material parameters for molybdenum.

Vacancy formation energy (E^f)	3.0 eV
Vacancy migration energy (E^m)	1.62 eV
Vacancy diffusivity (D_0)	13 nm^2/ps
Surface tension (γ_s)	2.05 J/m^2
Lattice constant (a_0)	3.1 Å
Atomic volume (Ω)	14.9 Å^3
Grid size (l)	1.0 Å
Time step (τ)	10^{-15} s

evolution is not affected by the vacancy emission from the void. Consequently, in considered case, the void growth rate of PFM cannot be modified by varying the surface tension as in other studies [15,29]. It is well known that the phase-field approach is a continuum mesoscale modeling apparatus that discards the discrete atomic nature of materials [39,40]. Accordingly, the equations of SBA and Eq. (7) (the PFM) are numerically solved in the spherical domain discretized along the radial direction with a uniform grid size $l \sim 1$ Å [18,28,39,41]. Taking a time step τ, single void evolution herein is emulated to a duration of $t \sim 10^{-4}$ s with $t \gg t_R$, where $t_R \sim R_{init}^2/2D$ is the characteristic time (or relaxation time) required for the formation of the steady diffusion field. All of the simulation and material parameters are listed in Table 1 [15,42].

In current phase-field model, the vacancy concentration will significantly vary across the interface. For the sake of accuracy and the convergence, an explicit second order finite-difference approach with a second order backward time-stepping technique is used in numerical solving process. The difficulty of selecting the optimal grid size arises then, which requires including at least one grid point located inside the interface field. The minimal interface width is therefore pre-evaluated using Eq. (22), which helps selecting the grid size used in all the subsequent cases. In this work, we have studied the effect of the grid size on the void dynamic first (not shown). Three values of l are selected out based on the estimation from Eq. (22) which are 0.147 nm (from Ref. [15]), 0.1 nm and 0.065 nm. It is found that if the grid size satisfies the former condition, the steady growth rates become independent of the grid size (within 0.5%). A smaller grid size l can contribute to obtaining more details in the diffuse interface however. In this case, a smaller time-step is required, which leads to a large computational load. In the following, only the results with $l = 0.1$ nm are presented.

Various reduced bulk free energy densities $f[c]$ used in the subsequent simulations are shown in Fig. 2(a), under conditions of $T = 1100$ K and $c_0 = 10^{-7}$. It is seen that all of the curves show the double-well shape, i.e. two local minima at $c \approx c_e$, $c \approx 1$ and one maximum. Moreover, they overlap at low vacancy concentration in the small window, which means that these densities deviate from the condition of the ideal dilute solution at a relatively high vacancy concentration. Therefore the initial vacancy concentration in studied cases remains far away from the spinodal point, where the solution becomes intrinsically unstable. For free energy density types of Eq. (10), the amplitude of the potential height f_{max} significantly varies as functions of n. For example, f_{max} for $n = 5.0$ is almost three times of that in $n = 2.0$ case. In order to furthermore study the density's shape effect on the void evolution, one case using the formulation of Eq. (12) but scaled by a factor of 1.4 ($= f_{max}(n = 4.0)/f_{max}$(Eq. (12))) is also shown and called 'Mod. Eq. (12)', which has an identical f_{max} with the case $n = 4.0$ whereas their shapes and the positions of the local maximum are different. The corresponding values of $\varkappa$ and Δl are listed in Table 2, respectively, computed from Eqs. (17) and (22) for different f_{max}. In order to exactly reproduce the results of Ref. [15], special care is paid on the case using Eq. (12) where we assume the integration term $I = 1$ in the calculation of quantity $\varkappa$. Accordingly, substituting the functional form of $f[c]$ and the corresponding $\varkappa$ into the phase-field frameworks, the evolution of the vacancy concentration profile can be solved, from which the temporary void radius can be estimated using Eq. (8). And after a fast relaxation regime, the steady-state void growth rate Γ can be obtained from the increasing rate of the void radius.

Fig. 2(b) shows the steady-state growth rate ratio Γ/Γ_{RT} of the aforementioned cases as well as the sharp boundary approach to the prediction of the rate theory (see Eq. (1)) as functions of reduced initial (and boundary) concentrations c_0/c_e with $T = 1100$ K and $R_{init} = 1.02$ nm. First, quantitative matching of the void growth rate between the SBA and RT can be clearly seen for all conditions. Regarding the PFM, the case using Eq. (12) has successfully reproduced the results of Ref. [15], of which the void growth rates present considerable errors compared to the predictions of RT, especially at low initial vacancy concentration. Then the error generated by using Eq. (10) reduces with increasing parameter n, namely f_{max} (see Table 2). More importantly, such error between the PFM and RT is vanished while $n \geqslant 4.0$ whatever the initial vacancy concentration.

The effect of the free energy density's shape can then be distinguished from the case Mod. Eq. (12). It is hereby recalled that the potential height of Mod. Eq. (12) is the same with that of $n = 4.0$ case. And likewise, the corresponding steady void growth rate of Mod. Eq. (12) is consistent with the RT prediction and the error is within only 1% for all of the initial vacancy concentration cases. According to the data in Table 2 and the above results, the local maximum of the bulk free energy density and thus the interface width has a first order contribution on the void dynamics, regardless of the free energy density's shape. Back to the case using Eq. (12), although f_{max}(Eq. (12)) is close to $f_{max}(n = 3.0)$, their growth rates present large differences. This demonstrates that the gradient energy coefficient $\varkappa$ also plays an essential role, and in this regard, the interface width seems to be the most appropriate criteria to characterize the void dynamic. Further evidence is that the steady growth rate obtained using Eq. (12) is between those obtained in the cases of $n = 2.0$ and $n = 2.5$, while its corresponding interface width exactly falls in a range of these two cases.

Examinations are also performed on the variation of the initial void radius and temperature. In the following, two typical values of n (2.0 and 4.0) for the density form of Eq. (10) are selected out, which correspond to cases exhibiting the largest interface width and the critical interface width, respectively. All of the curves in Fig. 2(c) present a similar trend, where the growth rate is inversely proportional to the void radius as predicted by Eq. (1) for $L \gg R$. And then within the studied temperature range, the vacancy emission from the void is limited. Hence, the temperature dependency of the void growth rate shown in Fig. 2(d) is entirely determined by the vacancy diffusion coefficient, which agrees again with the prediction of Eq. (1). Interestingly, regardless of the simulation conditions, the results of the PFM with smaller Δl present better agreements with the predictions of the SBA and RT. In conclusion, despite the shape of $f[c]$, the desired void growth rate can be obtained while $\Delta l \leqslant 1.5$ Å. More generally, to accurately reproduce the void dynamic as predicted by the SBA and RT, an appropriate potential barrier must be selected at first and then the corresponding gradient energy coefficient $\varkappa$ need to be determined using Eq. (17) to ensure that the estimated interface width is smaller than a critical value, e.g. $\Delta l \leqslant 1.5$ Å for the studied example.

And to obtain details of the diffuse interface, the vacancy concentration profiles $c(r)$ after the formation of the steady diffuse field are plotted in Fig. 3 at $T = 1100$ K with $c_0 = 10^{-7}$ and $R_{init} = 1.02$ nm, as well as the result of SBA for comparisons. The shaded region highlights the interface area. It should be noted that unlike the PFM, the SBA does not have a diffuse interface and the vacancy concentration inside the void is zero. Therefore, the comparison can be done only outside of the void. It is seen that out of the diffuse field, all of the vacancy concentration distributions of the PFM perform well the characteristic r^{-1} behavior, which is consistent with the SBA profile.

With a global view of PFM profiles, $c(r)$ decreases from unity in the void to almost zero in the matrix through a narrow diffuse region. It is obvious that a relatively wider interface is formed in the cases of Eq.

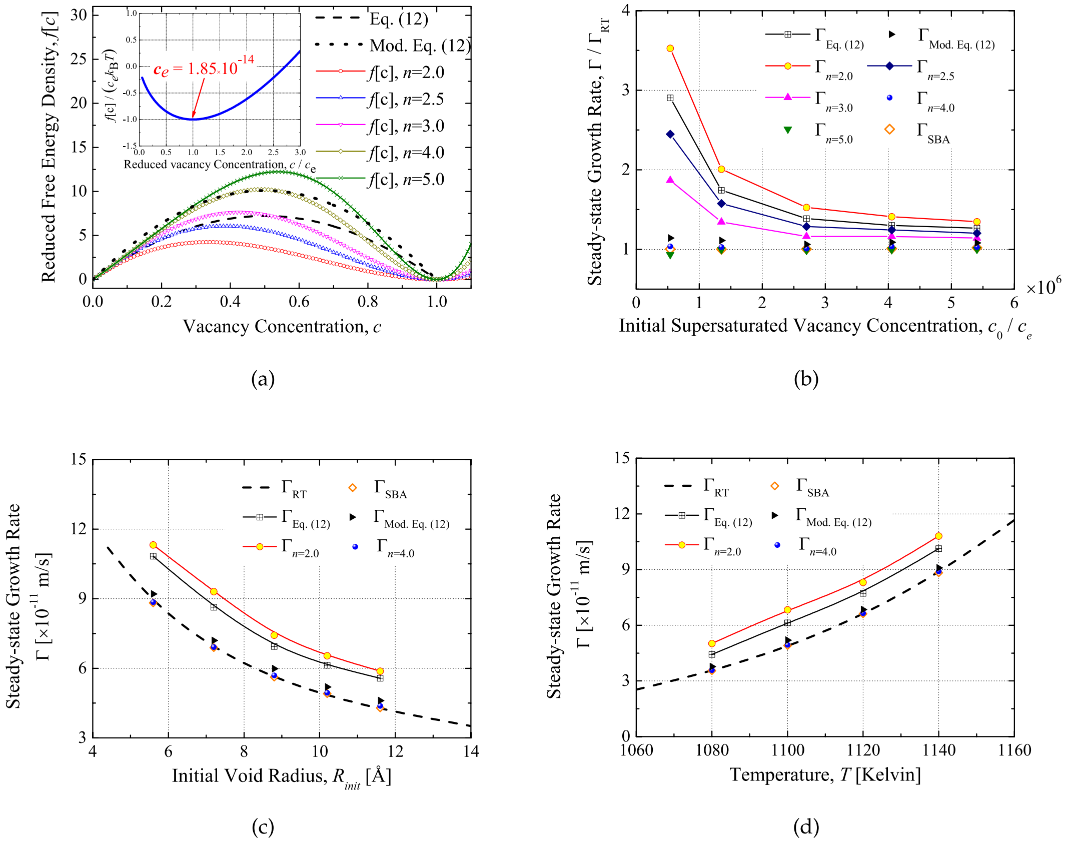

(a)

(b)

(c)

(d)

Fig. 2. (a) The dimensionless bulk free energy density for $T = 1100$ K and $c_0 = 10^{-7}$, with details near c_e inserted. (b) Steady growth rate ratio Γ/Γ_{RT}, with Γ_{RT} representing the result of rate theory, as functions of the reduced initial (and boundary) concentration c_0/c_e for $T = 1100$ K and $R_{init} = 1.02$ nm. (c) Steady growth rate Γ as functions of the initial void radius for $T = 1100$ K and $c_0 = 10^{-7}$. (d) Steady growth rate Γ as functions of the temperature for $c_0 = 10^{-7}$ and $R_{init} = 1.02$ nm.

Table 2
Characteristic parameters with different bulk free energy density formulations for $T = 1100$ K and $c_0 = 10^{-7}$.

	Eq. (12)	Mod. Eq. (12)	$n = 2.0$	$n = 2.5$	$n = 3.0$	$n = 4.0$	$n = 5.0$
f_{max}	7.32	10.25	4.11	6.10	7.63	10.25	12.23
$\varkappa$ (Å)	10.05	4.72	8.13	5.82	5.21	4.43	4.02
Δl (Å)	3.71	1.47	4.01	2.35	1.89	1.38	1.15

(12) and $n = 2.0$. Whereas in $n = 4.0$ and Mod. Eq. (12) cases, $c(r)$ profile yields a sharp interface similar to the SBA, with a characteristic width less than one lattice constant, despite its diffuse character. Compared to the interface width estimated from Table 2 that is derived from the static planar condition, the relative data is in good agreement with the graphical observation. For instance, 5 grid points can be observed in the diffusive field of the case $n = 2.0$, which corresponds to $\Delta l = 4.01$ Å listed in the table. In $n = 4.0$ and Mod. Eq. (12) cases, only 2.5–3 grid points are present in each diffuse field.

The precise evaluation of the interface width from the simulations is generally difficult. A simple method $\nabla c(r)|_{c=0.5} = -1/\Delta l$ is alternatively adopted in this work. The results of the interface width estimated from $c(r)$ as functions of f_{max}^{-1} are shown in Fig. 4 and compared to the analytic predictions based on Eq. (22), where the linear relation confirms our analysis in Section 2. Indeed, the sharpness of the diffuse interface is a direct result of the behavior of the thermodynamic potential in the ideal dilute solution limit [32]. A smaller f_{max} will accelerate the deviation of the potential from this limit (deviating at lower vacancy concentration), and thus induces a wider interface. Then a wider interface is achieved by introducing more material into such field to decrease the contribution of the gradient energy term, which makes the interface more diffuse. Therefore, changing the barrier of the free energy density will affect the diffusivity of the interface and then the void dynamic.

It is known that the successful development of the phase-field models for the phase transition dynamic requires the numerical matching of their results to the SBA or RT predictions. As widely adopted in other studies, adjusting some material parameters such as the surface tension [15] and the interface mobility [43,44] or even roughly tuning the gradient energy coefficient can help to bring about the desired results. However, the fidelity of those methods must be further justified. Especially for the problem of void nucleation and growth, the introduction of the diffuse interface in the PFM only slightly affects the interfical tension because of the low vacancy concentration in the matrix [45], even under in-reactor conditions, which is always far away from the spinodal point (see Fig. 2(a)). Moreover, as discussed in Ref. [33], directly fitting the gradient energy coefficient may cause discrepancies in the void nucleation probability deviating from the classical nucleation theory. Fig. 4 thus presents its potential in validating the characteristic parameters of the void nucleation and growth process, where the obtained interface width should follow the linear relation with respect to f_{max}^{-1}, and at the same time is smaller than a critical value. In this regard, based on Eq. (22), using the appropriate free energy density coupled with the gradient energy coefficient always provides an available and reliable path to correctly and accurately model the void dynamic.

Finally, the above results also demonstrate that for a fixed temperature, it is reasonable to treat the gradient energy coefficient as a constant independent of void size under the real experimental conditions, regardless of the bulk free energy density forms. Although the void dynamic needs to be performed in an ultrafine spatial scale, this phase-field model is still beneficial for studying the void nucleation and growth problem, where some theoretical analysis can be alternatively

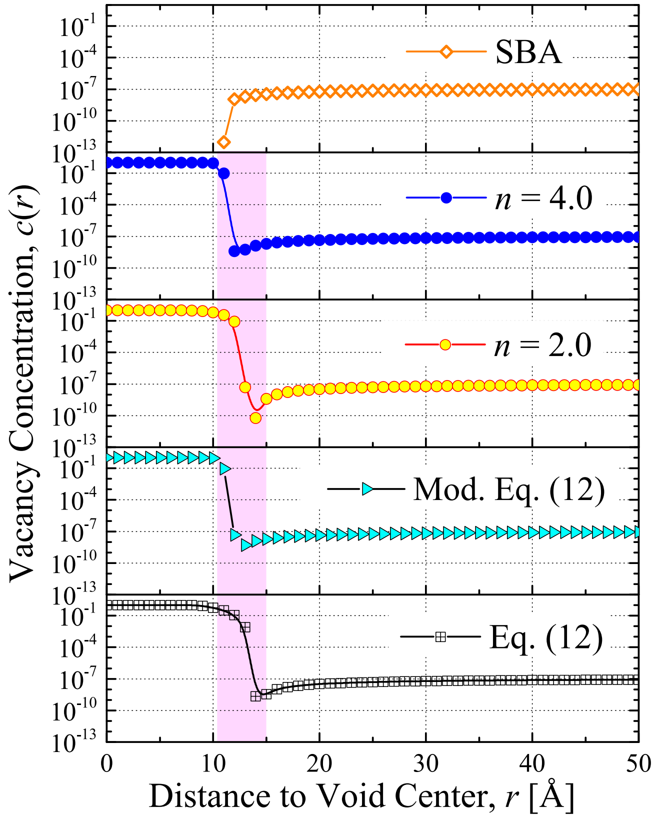

Fig. 3. Vacancy concentration profiles after $t = 10^{-4}$ s with different bulk free energy density formulations for $c_0 = 10^{-7}$, $R_{init} = 1.02$ nm and $T = 1100$ K, compared with the result of SBA. Only these grids where $r \leqslant 50$ Å are shown for purposes of more clearly illustrating the diffuse interface (the shaded region).

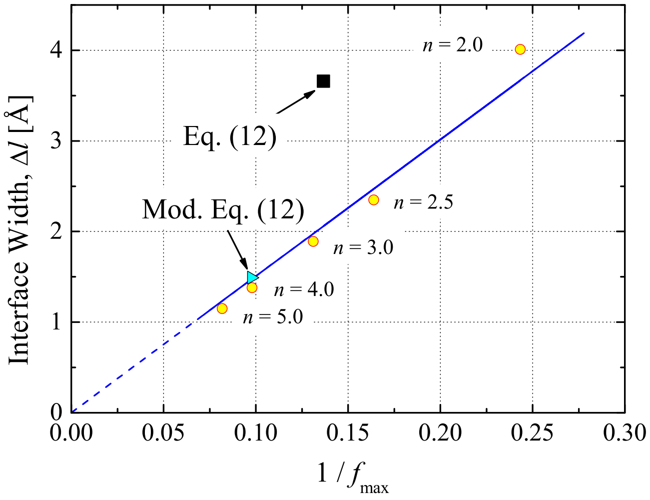

Fig. 4. The interface width Δl as functions of the inverse of the reduced bulk free energy density barrier. The scatters are estimations from the PFM simulation and the solid line is the prediction of Eq. (22) with dashed line extrapolating to the origin to show the linear relation.

done in the planar interface case. Moreover, a possible method for modelling the evolution of void ensembles in such fine spatial scale is matched asymptotic expansion to relate the PFM to the SBA by smearing out the interface [19]. The findings reported here, for instance the expressions of κ-coefficient and the interface width, may thus be applied to simplifying the corresponding matched asymptotic analysis.

4. Conclusion

An improved phase-field model using the vacancy concentration as the single order parameter is developed in this work to treat the problem of void nucleation and growth. The purpose of this study is to obtain the accurate void growth rate benchmarked by the value calculated from the sharp boundary approach and rate theory. Based on the quantitative analysis and the simulation example of a single void evolution, we found that:

- The expression of the gradient energy coefficient κ is simplified without any other assumptions against the classical nucleation theory. The expression of the interface width as functions of the gradient energy coefficient and the local maximum is then analytically derived from the planar interface case, which can be used to adjust the void dynamic;
- The interface width has a first order contribution on the void dynamic. Using the former relation, the accurate void growth rate can be obtained by tuning f_{max} to satisfy that the interface width is smaller than a critical value.

This work will not only help to construct the appropriate formulation of the bulk free energy density, but also provide an easy path to compute the corresponding gradient energy coefficient and to select the grid size and time step according to the pre-estimated interface width.

CRediT authorship contribution statement

Yang Li: Conceptualization, Data curation, Formal analysis, Investigation, Methodology, Software, Visualization, Writing - original draft. **Decai Ma:** Funding acquisition, Supervision, Validation, Writing - review & editing. **Biao Wang:** Funding acquisition, Project administration, Resources, Validation.

Acknowledgment

This work was supported by the National Natural Science Foundation of China (NSFC) (Nos. 11372361, 11302268, 11232015, 11472321, 11572355), to which the authors are thankful. Authors also gratefully acknowledge discussions with D.R. Christian Robertson.

References

[1] A.D. Braislford, R. Bullough, Void growth and its relation to intrinsic point defect properties, J. Nucl. Mater. 69–70 (Suppl. C) (1978) 434–450.

[2] S.I. Golubov, B.N. Singh, H. Trinkaus, Defect accumulation in fcc and bcc metals and alloys under cascade damage conditions – towards a generalisation of the production bias model, J. Nucl. Mater. 276 (1) (2000) 78–89.

[3] V.I. Dubinko, S. Hu, Y. Li, C.H.H. Jr, R.J. Kurtz, Dislocation vs. production bias revisited with account of radiation-induced emission bias. I. Void swelling under electron and light ion irradiation, Philos. Mag. 92 (33) (2012) 4113–4150.

[4] G.S. Was, Fundamentals of Radiation Materials Science: Metals and Alloys, Springer, 2016.

[5] T. Marieb, P. Flinn, J.C. Bravman, D. Gardner, M. Madden, Observations of electromigration induced void nucleation and growth in polycrystalline and near bamboo passivated Al lines, J. Appl. Phys. 78 (2) (1995) 1026–1032.

[6] M.P. Surh, J.B. Sturgeon, W.G. Wolfer, Void nucleation, growth, and coalescence in irradiated metals, J. Nucl. Mater. 378 (1) (2008) 86–97.

[7] Y. Fan, A. Kushima, S. Yip, B. Yildiz, Mechanism of void nucleation and growth in bcc Fe: atomistic simulations at experimental time scales, Phys. Rev. Lett. 106 (12) (2011) 125501 .

[8] N. Aravas, The analysis of void growth that leads to central bursts during extrusion, J. Mech. Phys. Solids 34 (1) (1986) 55–79.

[9] V.S. Neustroev, F.A. Garner, Very high swelling and embrittlement observed in a Fe-18cr-10ni-Ti hexagonal fuel wrapper irradiated in the BOR-60 fast reactor, J. Nucl. Mater. 378 (3) (2008) 327–332.

[10] B.Z. Margolin, I.P. Kursevich, A.A. Sorokin, A.N. Lapin, V.I. Kokhonov, V.S. Neustroev, Embrittlement and fracture toughness of highly irradiated austenitic steels for vessel internals of WWER type reactors. Part 1. Relation between irradiation swelling and irradiation embrittlement. Experimental results, Strength Mater. 41 (6) (2009) 593.

[11] B. Margolin, A. Sorokin, V. Shvetsova, A. Minkin, V. Potapova, V. Smirnov, The

radiation swelling effect on fracture properties and fracture mechanisms of irradiated austenitic steels, J. Nucl. Mater. 480 (2016) 52–68.
[12] A.D. Brailsford, R. Bullough, The rate theory of swelling due to void growth in irradiated metals, J. Nucl. Mater. 44 (2) (1972) 121–135.
[13] S.J. Zinkle, G.S. Was, Materials challenges in nuclear energy, Acta Mater. 61 (3) (2013) 735–758.
[14] A. Gokhman, J. Boehmert, A kinetics study of vacancy cluster evolution under VVER-type reactor condition, Radiat. Eff. Defects Solids 158 (7) (2003) 499–511.
[15] Z.H. Xiao, A.A. Semenov, C.H. Woo, S.Q. Shi, Single void dynamics in phase field modeling, J. Nucl. Mater. 439 (1–3) (2013) 25–32.
[16] J.W. Gibbs, The Scientific Papers of J. Willard Gibbs, Longmans, Green and Company, 1906 vol. 1.
[17] J.L. Katz, H. Wiedersich, Nucleation of voids in materials supersaturated with vacancies and interstitials, J. Chem. Phys. 55 (3) (1971) 1414–1425.
[18] T. Hochrainer, A. El-Azab, A sharp interface model for void growth in irradiated materials, Philos. Mag. 95 (9) (2015) 948–972.
[19] H. Emmerich, Advances of and by phase-field modelling in condensed-matter physics, Adv. Phys. 57 (1) (2008) 1–87.
[20] Y. Li, S. Hu, X. Sun, F. Gao, C.H. Henager, M. Khaleel, Phase-field modeling of void migration and growth kinetics in materials under irradiation and temperature field, J. Nucl. Mater. 407 (2) (2010) 119–125.
[21] P.C. Millett, S. Rokkam, A. El-Azab, M. Tonks, D. Wolf, Void nucleation and growth in irradiated polycrystalline metals: a phase-field model, Modell. Simul. Mater. Sci. Eng. 17 (6) (2009) 064003 .
[22] S. Hu, C.H. Henager, Phase-field modeling of void lattice formation under irradiation, J. Nucl. Mater. 394 (2) (2009) 155–159.
[23] S.Y. Hu, C.H. Henager, Phase-field simulation of void migration in a temperature gradient, Acta Mater. 58 (9) (2010) 3230–3237.
[24] P.C. Millett, A. El-Azab, S. Rokkam, M. Tonks, D. Wolf, Phase-field simulation of irradiated metals: part I: void kinetics, Comput. Mater. Sci. 50 (3) (2011) 949–959.
[25] D.O. Kharchenko, V.O. Kharchenko, Y.M. Ovcharenko, O.B. Lysenko, I.A. Shuda, L. Wu, R. Pan, Phase field modelling voids nucleation and growth in binary systems, Condens. Matter Phys. 21 (1) (2018) 13002.
[26] M. Imada, Void lattice formation-spinodal decomposition of vacancies, J. Phys. Soc. Jpn. 45 (5) (1978) 1443–1448.
[27] N. Wang, S. Rokkam, T. Hochrainer, M. Pernice, A. El-Azab, Asymptotic and uncertainty analyses of a phase field model for void formation under irradiation, Comput. Mater. Sci. 89 (2014) 165–175.
[28] M.R. Tonks, A. Cheniour, L. Aagesen, How to apply the phase field method to model radiation damage, Comput. Mater. Sci. 147 (2018) 353–362.
[29] K. Ahmed, A. El-Azab, An analysis of two classes of phase field models for void growth and coarsening in irradiated crystalline solids, Mater. Theory 2 (1) (2018) 1.
[30] A.A. Semenov, C.H. Woo, Phase-field modeling of void formation and growth under irradiation, Acta Mater. 60 (17) (2012) 6112–6119.
[31] H.-C. Yu, W. Lu, Dynamics of the self-assembly of nanovoids and nanobubbles in solids, Acta Mater. 53 (6) (2005) 1799–1807.
[32] A.A. Semenov, C.H. Woo, Interfacial energy in phase-field emulation of void nucleation and growth, J. Nucl. Mater. 411 (1–3) (2011) 144–149.
[33] A.A. Semenov, C.H. Woo, Modeling void development in irradiated metals in the phase-field framework, J. Nucl. Mater. 454 (1–3) (2014) 60–68.
[34] J.W. Cahn, J.E. Hilliard, Free energy of a nonuniform system. I. Interfacial free energy, J. Chem. Phys. 28 (2) (1958) 258–267.
[35] J.W. Cahn, J.E. Hilliard, Free energy of a nonuniform system. III. Nucleation in a two component incompressible fluid, J. Chem. Phys. 31 (3) (1959) 688–699.
[36] J.W. Cahn, On spinodal decomposition, Acta Metall. 9 (9) (1961) 795–801.
[37] V.K. Sikka, J. Moteff, Stability of the defect state in neutron-irradiated molybdenum, Nucl. Technol. 22 (1) (1974) 52–65.
[38] V.K. Sikka, J. Moteff, Damage in neutron-irradiated molybdenum: (I). Characterization of as-irradiated microstructure, J. Nucl. Mater. 54 (2) (1974) 325–345.
[39] A. El-Azab, K. Ahmed, S. Rokkam, T. Hochrainer, Diffuse interface modeling of void growth in irradiated materials. mathematical, thermodynamic and atomistic perspectives, Curr. Opin. Solid State Mater. Sci. 18 (2) (2014) 90–98.
[40] K. Ahmed, C. Yablinsky, A. Schulte, T. Allen, A. El-Azab, Phase field modeling of the effect of porosity on grain growth kinetics in polycrystalline ceramics, Modell. Simul. Mater. Sci. Eng. 21 (6) (2013) 065005 .
[41] J. Clayton, P. Chung, M. Grinfeld, W. Nothwang, Kinematics, electromechanics, and kinetics of dielectric and piezoelectric crystals with lattice defects, Int. J. Eng. Sci. 46 (1) (2008) 10–30.
[42] Ehrhart P. Properties and interactions of atomic defects in metals and alloys. vol. 25 of landolt-börnstein, new series iii, ch. 2. 88; 1991.
[43] M. Mecozzi, M. Militzer, J. Sietsma, S. van der Zwaag, The role of nucleation behavior in phase-field simulations of the austenite to ferrite transformation, Metall. Mater. Trans.A 39 (6) (2008) 1237–1247.
[44] M.M. Tavakoli, R. Tavakoli, P. Davami, H. Aashuri, A quantitative approach to study solid state phase coarsening in solder alloys using combined phase-field modeling and experimental observation, J. Comput. Electron. 13 (2) (2014) 425–431.
[45] C.K. Bagdassarian, D.W. Oxtoby, Crystal nucleation and growth from the undercooled liquid: a nonclassical piecewise parabolic free-energy model, J. Chem. Phys. 100 (3) (1994) 2139–2148.